DISTRIBUTION STATEMENT A. Approved for public release; distribution is unlimited.

Scattering of Acoustic Waves from Ocean Boundaries

Marcia J. Isakson
Applied Research Laboratories
The University of Texas at Austin, TX 78713-8029
phone: (512)835-3790 fax: (512)835-3259 email: misakson@arlut.utexas.edu

Award Number: N00014-12-1-0137
http://www.arlut.utexas.edu

LONG-TERM GOALS

Development of a physical model of high-frequency acoustic interaction with the ocean floor, including penetration through and reflection from smooth and rough water/sediment interfaces, scattering from the interface roughness and volume heterogeneities and propagation within the sediment. The model will aid in the detection and classification of buried mines and improve SONAR performance in shallow water.

OBJECTIVES

1) Determination of the correct physical model of acoustic propagation through ocean sediments and scattering from sediment interfaces through the analysis of in situ measurements.
2) Development of predictive models that can account for the all of the physical processes and variability of acoustic propagation and scattering in ocean environments with special emphasis on propagation in shallow water waveguides and scattering from ocean sediments.
3) Development of the new experimental techniques to measure geo-acoustic parameters in the ocean.

APPROACH

1) *Finite Element Modeling for Range Dependent Waveguides*: Finite element modeling is applied to a waveguide with measured range dependent geo-acoustic parameters in order to calculate transmission loss and reverberation. Two different approaches to the three-dimensional problem are taken: axially symmetric models and longitudinally invariant modeling.
2) *Analysis of Normal Incidence Bottom Loss Measurements for Range Dependent Geoacoustic Parameters:* Bottom loss data from 5 – 30 kHz were collected as part of the Target and Reverberation Experiment 2013 (TREX13). These data were analyzed and range dependent geoacoustic parameters were derived for the TREX reverberation site including bottom loss and scattering. The data were compared with multibeam sonar data taken at the same site.
3) *Measurements of Bottom Loss, Sediment Structure and Interface Roughness at the Glider Sensors and payloads for Tactical characterization of the Environment (GLISTEN15) Experiment:* Normal incidence bottom loss measurements from 5-20 kHz and interface roughness data were collected using an ROV platform as part of the GLISTEN experiment.

WORK COMPLETED

Finite Element Modeling for Range Dependent Waveguides

A finite element model of propagation and scattering was calculated based on the domain shown in Fig. 1 and the geoacoustic parameters in Table 1. The parameters were derived from measurements taken on-site. Since at this time, full three-dimensional models were outside the capability of available computers, two approaches to the problem were taken. The first approach was to compute the waveguide as axially symmetric. The second approach used an plane wave integral transform method which assumes invariance in one spatial dimension of the waveguide. In this case, the dimension is perpendicular to the domain shown in Fig. 1. These solutions were compared with a range independent solution.

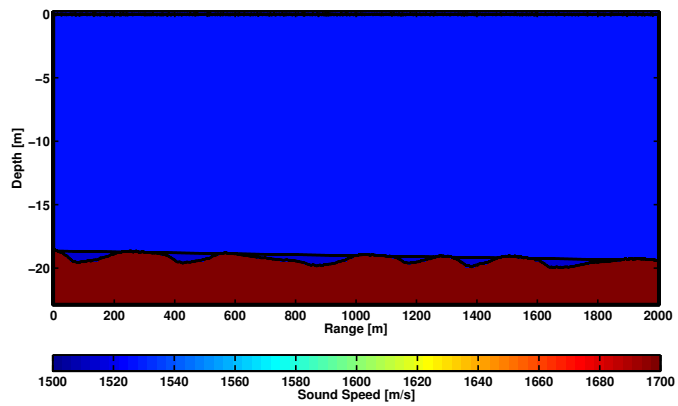

Figure 1: The domain used for the finite element model of TREX Propagation and Reverberation.

Layer	Water	Mud	Sand
Compressional Speed [m/s]	1525	1514	1769
Compressional Att. [dB/□]	Fran.-Garr.	0.08	0.3
Roughness Spectrum	Pierson-Moskowitz	Flat	Power-law (von Karman)
RMS Roughness [m]	0.045	0.0	0.003
Density [kg/m^3]	1024	1228	2100

Table 1. Geoacoustic parameters used in the finite element model based on measurements taken on site.

Analysis of Normal Incidence Bottom Loss Measurements for Range Dependent Geoacoustic Parameters

Data taken at the Target and Reverberation Experiment in May 2013 were analyzed and compared with bathymetric and high frequency backscatter measurements taken on site by deMoustier and Kraft.

Although multiple data sets were taken, the bottom loss data shown in Fig. 2 were analyzed for initial bottom loss and scattering. Fig. 3 shows the match-filtered data as a function of depth, which was determined from the sampling frequency and measured water sound speed and the ping number. Each ping had an associated latitude and longitude since the ROV was tracked using an ultrashort –baseline (USB) acoustic tracking system. This allowed the ROV data to be directly compared to the multibeam survey (MBS). The tracking system also recorded the depth of the ROV and with the bathymetry measured from the MBS, the range of the bottom return could be predicted. This is shown with the heavy black line in Fig. 3. The bottom loss was measured by considering the initial bottom return relative to a calibrated return taken in the laboratory from a air/water interface. The range of this return was determined by considering the maximum of the signal shown with the blue line. Also, considered was the scattering. Its relative value was estimated by measuring the energy in the signal for a fixed time after the initial return. The fixed time interval is denoted with the white lines in Fig. 3. These measurements are referred to as "coda" energy.

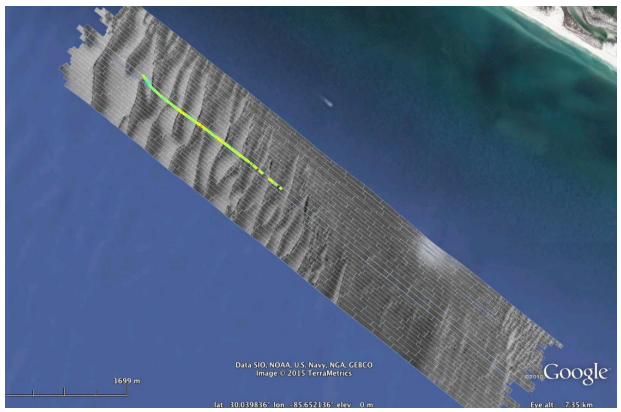

Figure 2: The location of the bottom loss measurements relative to the backscatter of the multibeam survey.

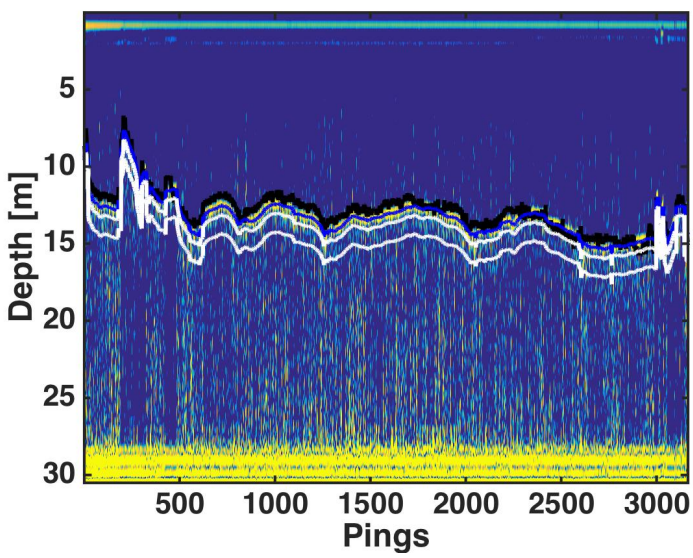

Figure 3: The magnitude of the match-filtered data of each ping in the survey shown in Fig. 2.

Measurements of Bottom Loss, Sediment Structure and Interface Roughness at the Glider Sensors and payloads for Tactical characterization of the Environment (GLISTEN15) Experiment

ARL:UT also participated in the Fliger Sensors and payloads for Tactical characterisation of the Environment (GLISTEN15) experiment conducted in August and September of 2015 off the west coast of Italy. Three data products were produced by ARL: video surveillance of the ocean bottom, normal-incidence bottom loss data which is also an indicator of scattering and layering and laser line profiling data. The expereimental setup is shown in Fig. 4.

The data collected by the ARL:UT system will aid in modeling the low-frequency propagation data taken by CMRE as part of the experiment. It is expected that ARL:UT will produce a finite element model of the propagation to understand the influence of range and depth dependent geoacoustic paramters. To those aims, data was taken along the two propagation paths of the experiment, the north-south track which was relatively range-independent in bathymetry and the east-west track which was range dependent in bathymetry with more than a 200 m depth change. The locations of the ROV deployments are shown in purple relative to the propagation paths in Fig. 5. In the figure, north is toward the top.

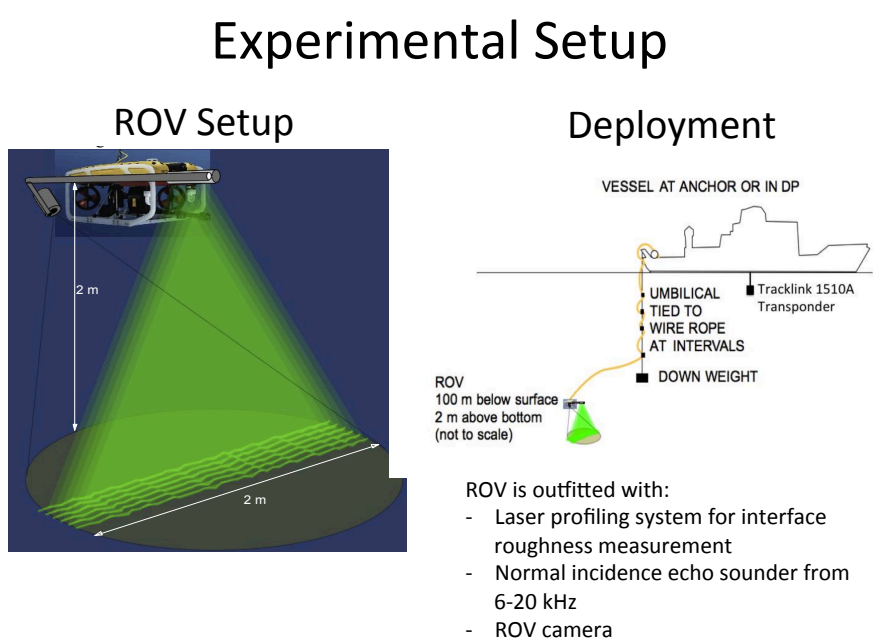

Figure 4: The experimental set-up for the ARL:UT ROV for the GLISTEN experiment.

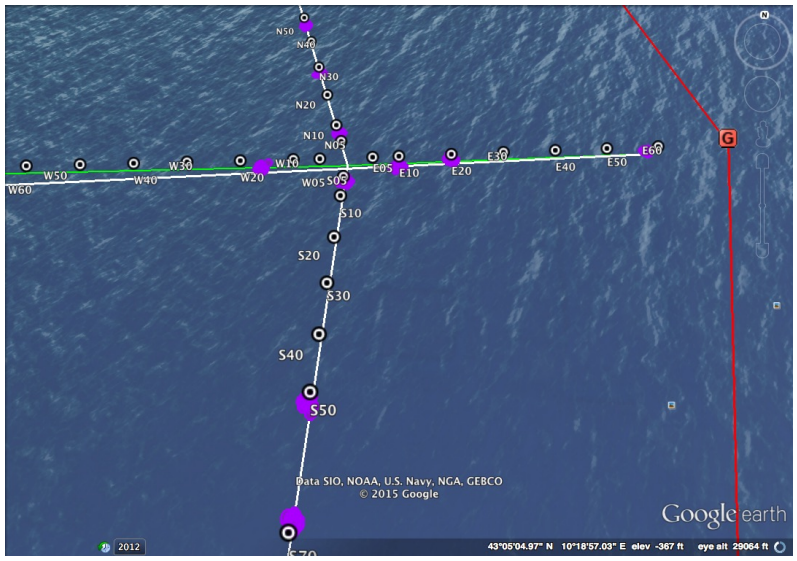

Figure 5: Locations of data collection for the ARL:UT ROV (shown in purple) relative to the propagation paths for the GLISTEN experiment.

RESULTS

Finite Element Modeling for Range Dependent Waveguides

The finite element propagation model was compared to two different types of models at two different frequencies to assess the effects of range dependence on transmission loss. Shown in Fig. 6 is the axi-symmetric FEM compared with OASES which assumed range independent parameters and simple cylindrical spreading. The longitudinally invariant model was not run at this frequency due to the large number of out-of-plane wavenumbers required. The left panel shows the models at 1 m increments while the right panel shows the range-averaged energy. The range-dependent finite element model shows significantly more loss than the range-independent case.

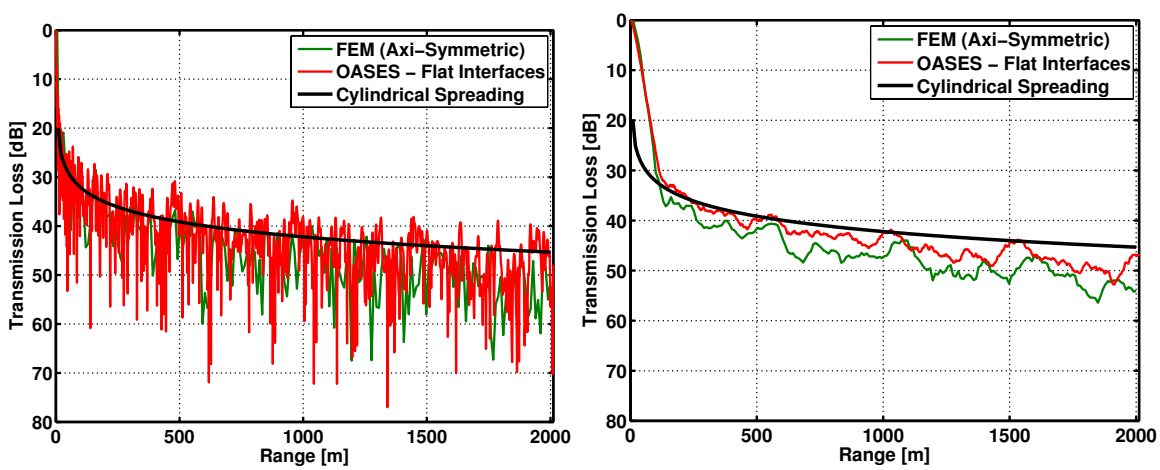

Figure 6: Finite element propagation loss for 1900 Hz over domain shown in Fig. 1. In the right panel, the data has been averaged over 100 m increments to show the change in level.

Propagation loss at 500 Hz was also calculated using the finite element model. The results are shown in Fig. 7. In this case, the longitudinally invariant model was also calculated. This geometry is more suitable to the physical environment since the sand waves were relatively longitudinal. The left panel shows the data averaged over 200 m increments. In this case, the axi-symmetric and range-independent cases (as shown by the OASES model) are largely in agreement. However, the longitudinally invariant finite element model indicates additional loss likely due to out of plane scattering by the sand waves.

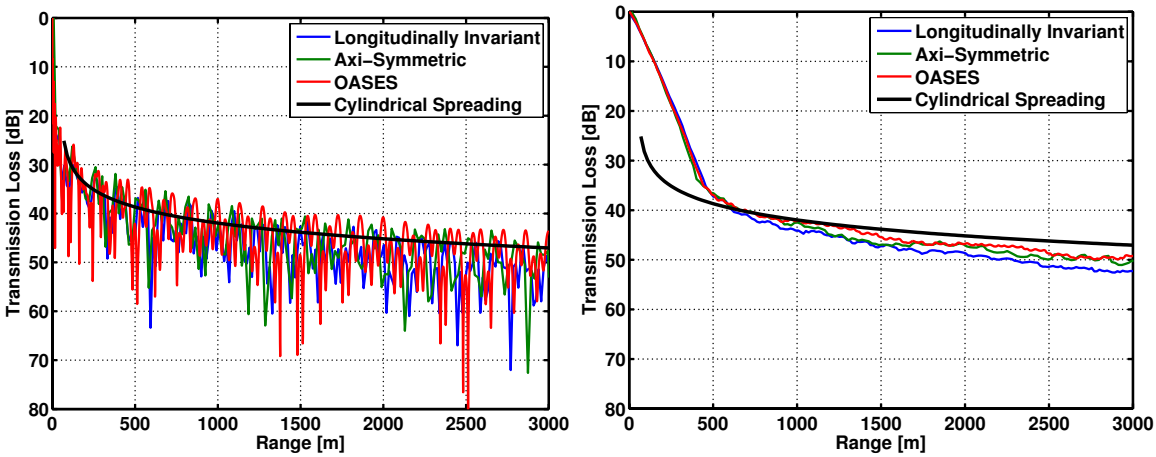

Figure 7: Propagation model for 500 Hz over domain shown in Fig. 1. The longitudinally invariant model and axi-symmetric model are calculated using finite elements. In the right panel, the data has been averaged over 100 m increments to show the change in level.

Lastly, low-frequency model of reverberation was calculated for 100 Hz using the axi-symmetric finite element model and the longitudinally invariant model. The results are shown in Fig. 8. Although the axi-symmetric model is much less computationally intensive than the longitudinally invariant model, it is contaminated by backwards propagating cylindrical waves. In the case of propagation, these are much lower than the forward going energy and do not distort the result as drastically. However, for reverberation, they are dominant and therefore, the axi-symmetric model is unsuitable for reverberation modeling in which the geometry is longitudinal such as the case with sand ripples.

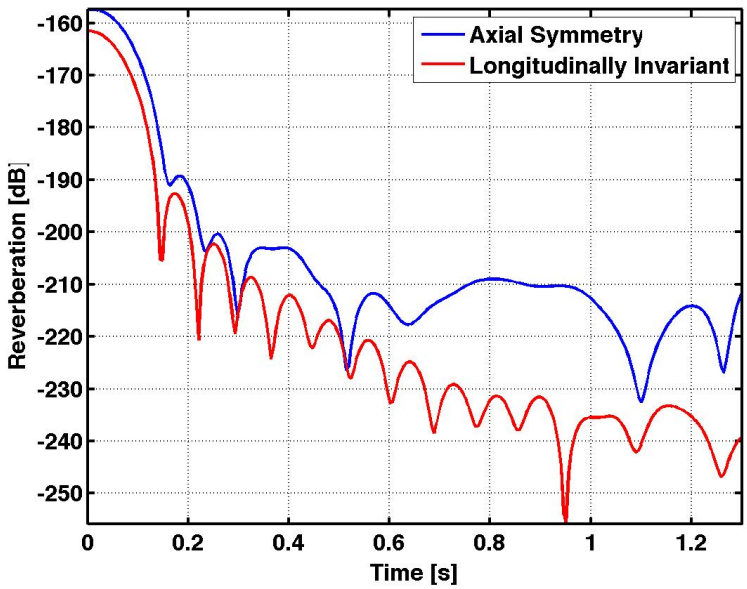

Figure 8: Finite element model of reverberation calculated at a center frequency of 500 Hz over the domain shown in Fig. 1.

Analysis of Normal Incidence Bottom Loss Measurements for Range Dependent Geoacoustic Parameters

The bottom loss and coda energy data derived from measurements at the locations shown in Fig. 2 were compared with the depth and backscatter from the MBS. Shown in Fig. 9 is the bottom loss data compared to the depth (right panel) and the backscatter (left panel). There is not a clear correlation between the bottom loss which at these frequencies can be related to sediment type and the bathymetry or backscatter. This may have implications for sediment transport. Conversely, the coda energy is compared to the depth (right panel) and backscatter (left panel) in Fig. 10. Here a clear correlation is seen which indicates that scattering is the dominate different in the peaks and troughs at the TREX site and that scattering is also the main mechanism behind the large variations in backscattering from the MBS survey.

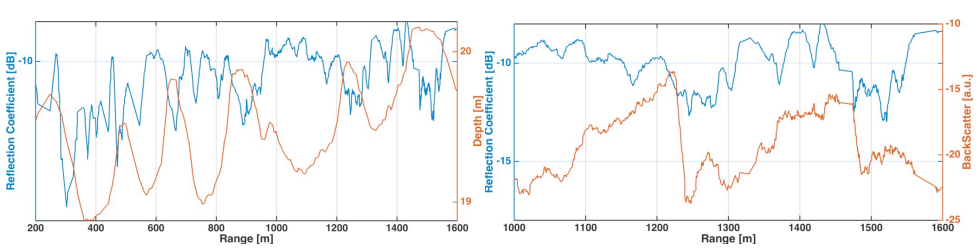

Figure 9: Bottom loss for the TREX track shown in Fig. 2 compare with MBS values of bathymetry (right panel) and backscatter (left panel).

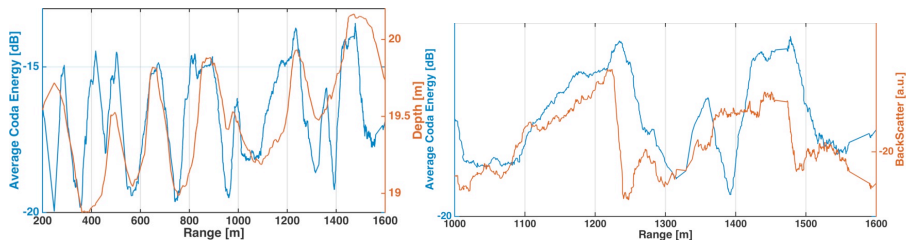

Figure 10: Coda energy for the TREX track shown in Fig. 2 compare with MBS values of bathymetry (upper panel) and backscatter (lower panel).

Measurements of Bottom Loss, Sediment Structure and Interface Roughness at the Glider Sensors and payloads for Tactical characterization of the Environment (GLISTEN15) Experiment

Since the GLISTEN sea test was so recent, only preliminary data analysis has been performed. Shown in Fig. 11 is a sample of the normal incidence bottom loss data. In the figure, a depth dependent structure is evident. The sediment was a mud and the volume inclusions, likely due to biology based on video data, are clearly visible. Also, a lower layer is visible over some of the area. These data have not yet been accurately assigned latitude and longitude based on a USB tracking system.

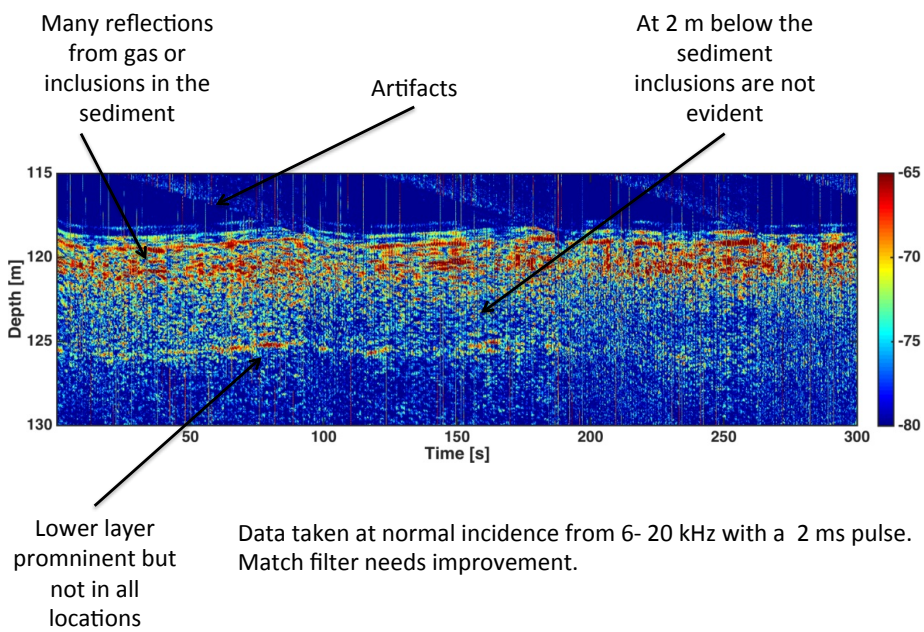

Figure 11: Preliminary bottom loss data from the GLISTEN experiment.

Shown in Fig. 12 is an example of the laser line profiling data. Note that the bottom consisted of many burrows. Brittle stars and anemones were present in the area based on video data. These laser lines will be analyzed to provide an estimate of the roughness spectrum.

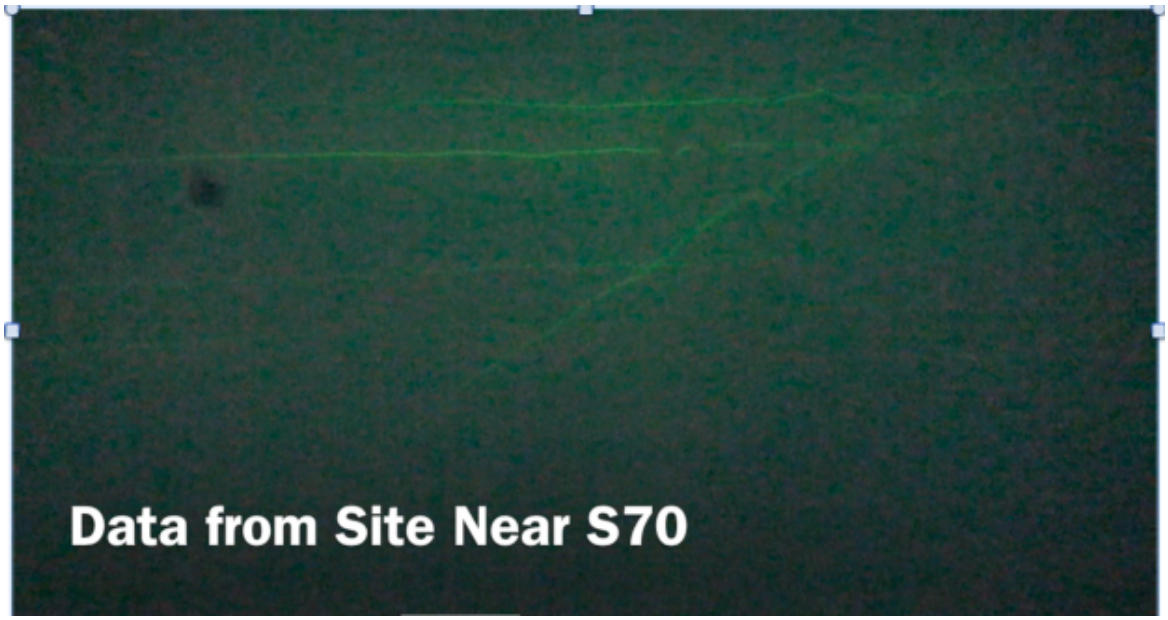

Figure 12: Laser line profiling data taken near site S70.

IMPACT/APPLICATIONS

The finite element reflection loss models could transition into a new high frequency and low frequency reflection loss (LFBL/HFBL) data curves for NAVO based on site-specific characteristics. It is also a benchmark for faster approximate methods of calculating propagation and scattering. The 3D LI model can be used to understand propagation and reverberation in complex environments. An understanding of normal incident reflection loss is critical to sediment characterization and mine burial prediction. The TREX13 measurements will serve as ground truth bottom loss and interface roughness measurements for reverberation modeling. GLISTEN data provide insight into the role of biology on acoustic propagation and scattering.

RELATED PROJECTS

Under the iPUMA and SSAM Sediment Environmental Estimation (iSSEE) program, this group is also developing sediment characterization algorithms for AUV sonars based on the measurements and models previously developed by this program. Additionally, the models developed in this research will be used to increase the fidelity of sonar trainers under the High Fidelity Active Sonar Trainer (HiFAST) program.

PUBLICATIONS

Bonomo, A.L., Chotiros, N. P. and Isakson, M. J., "On the validity of the effective density fluid model as an approximation of a poroelastic sediment layer," J. Acous. Soc. Am., 138, 748-757 (2015), DOI:http://dx.doi.org/10.1121/1.4926901.

Bonomo, A.L., Chotiros, N. P. and Isakson, M. J., "A comparison of finite element and analytic models of acoustic scattering from rough poroelastic interfaces," J. Acous. Soc. Am., 137, EL235-EL240 (2015), DOI:http://dx.doi.org/10.1121/1.4914947.

Ballard, M.S., Goldsberry, B.M. and Isakson, M.J. "Normal Mode Analysis of Three-Dimensional Propagation Over a Small-Slope Cosine Shaped Hill," J. Comp. Acous., 23(3) (2015), DOI:http://dx.doi.org/10.1142/S0218396X15500058

Isakson, M.J., Chotiros, N.P., Piper, J.N. and McNeese, A. "Acoustic Scattering from a Sandy Seabed at the Target and Reverberation Experiment 2013 (TREX13)," in Proc. IEEE/OES Acoustics in Underwater Geosciences Symposium, Rio de Janeiro, Brazil, July 2015.

PRESENTATIONS

Presenter:

Isakson, M.J., Chotiros, N.P., Piper, J.N. and McNeese, A. "Acoustic Scattering from a Sandy Seabed at the Target and Reverberation Experiment 2013 (TREX13)," in Proc. IEEE/OES Acoustics in Underwater Geosciences Symposium, Rio de Janeiro, Brazil, July 2015.

Isakson, M.J. and Chotiros, N.P. "Environmental Characterization from Normal Incidence Reflection Measurements," International Conference and Exhibition on Underwater Acoustics, Crete, Greece, June 2015.

Isakson, M.J. and Chotiros, N.P. "Finite Element Modeling for Three-Dimensional Propagation Benchmark Problems," International Conference and Exhibition on Underwater Acoustics, Crete, Greece, June 2015.

Isakson, M.J. and Chotiros, N.P. "Modeling three dimensional scattering from rough ocean boundaries using finite elements," J. Acous. Soc. Am., 137, 2420-2420 (2015), DOI:http://dx.doi.org/10.1121/1.4920828.

Isakson, M.J., Chotiros, N.P. and Lin, Y-T. "Three-dimensional underwater acoustic scattering from ocean boundaries: Proposed benchmark problems," J. Acous. Soc. Am., 137, 2420-2420 (2015), DOI:http://dx.doi.org/10.1121/1.4920829.

Isakson, M.J. and Chotiros, N.P., "Modeling reverberation in a complex environment with the finite element method," J. Acous. Soc. Am., 136, 2269-2269 (2014), DOI:http://dx.doi.org/10.1121/1.4900198.

Isakson, M. J. and Goldsberry, B. and Chotiros, N. P., "A three-dimensional, longitudinally-invariant finite element model for acoustic propagation in shallow water waveguides," J. Acous. Soc. Am., 136, EL206-EL211 (2014), DOI:http://dx.doi.org/10.1121/1.4890195.

Isakson, Marcia J. and Hamilton, Mark F. and Penrod, Clark S. and Pestorius, Frederick M. and Wilson, Preston S., "Underwater acoustics education at the University of Texas at Austin," J. Acous. Soc. Am., 136, 2188-2189 (2014), DOI:http://dx.doi.org/10.1121/1.4899930.

Co-Author:

Chotiros, N. P. and Isakson, M. J., "Fine-grained sediments from the poroelastic perspective," J. Acous. Soc. Am., 137, 2282-2282 (2015), DOI:http://dx.doi.org/10.1121/1.4920328.

Lin, Y-T and Isakson, M. J., "Three-dimensional underwater sound propagation: Proposed benchmark problems," J. Acous. Soc. Am., 137, 2420-2420 (2015), DOI:http://dx.doi.org/10.1121/1.4920830.

Bonomo, A. L., Chotiros, N. P. and Isakson, M. J., "An assessment of the effective density fluid model for backscattering from rough poroelastic interfaces." J. Acous. Soc. Am., 136, 2179-2179 (2014), DOI:http://dx.doi.org/10.1121/1.4899893.

Chotiros, N. P. and Isakson, M. J., "Comparison of measured acoustic reflection fluctuations and estimates based on roughness," J. Acous. Soc. Am., 137, 2391-2391 (2015), DOI:http://dx.doi.org/10.1121/1.4920703.

Bonomo, A. L., Chotiros, N. P. and Isakson, M. J., "An assessment of the effective density fluid model for scattering from poroelastic sediments with inclusions," J. Acous. Soc. Am., 137, 2391-2391 (2015), DOI:http://dx.doi.org/10.1121/1.4920705.

Chotiros, N. P., Isakson, M. J., Siliceo, O. E. and Abkowitz, P. M., "Roughness measurement by laser profiler and acoustic scattering strength of a sandy bottom," J. Acous. Soc. Am., 136, 2268-2268 (2014), DOI:http://dx.doi.org/10.1121/1.4900194.

Chandrika, U. K., Pallayil, V., Chotiros, N. and Isakson, M., "Seabed characterisation using a low cost digital thin line array: Results from the Target and Reverberation Experiments 2013," J. Acous. Soc. Am., 136, 2268-2268 (2014), DOI:http://dx.doi.org/10.1121/1.4900196.

Haberman, M. R., Hall, N. A., Hamilton, M. F., Isakson, M. J. and Wilson, P. S., "Graduate acoustics education in the Cockrell School of Engineering at The University of Texas at Austin," J. Acous. Soc. Am., 136, 2200-2200 (2014), DOI:http://dx.doi.org/10.1121/1.4899975.

Potty, G. R., Giard, J. L., Miller, J. H., Baxter, C., Isakson, M. J. and Goldsberry, B. M., "Shear wave inversion in a shallow coastal environment," J. Acous. Soc. Am., 136, 2156-2156 (2014), DOI:http://dx.doi.org/10.1121/1.4899797.